DISTRIBUTION STATEMENT A. Approved for public release; distribution is unlimited.

Predicting the Turbulent Air-Sea Surface Fluxes, Including Spray Effects, from Weak to Strong Winds

Edgar L Andreas
NorthWest Research Associates, Inc.
25 Eagle Ridge
Lebanon, New Hampshire 03766-1900
phone: (603) 448-3555 fax: (603) 448-3555 email: eandreas@nwra.com

Larry Mahrt
NorthWest Research Associates, Inc.
2171 NW Kari
Corvallis, Oregon 97330
phone: (541) 754-7501 fax: (541) 737-2540 email: mahrt@nwra.com

Contract Number: N00014-11-1-0073
http://www.nwra.com/

LONG-TERM GOALS

The goal is to investigate, through theory and by analyzing existing data, sea surface physics and air-sea exchange in winds that range from weak to hurricane strength. Ultimately, we want to develop unified parameterizations for the fluxes of momentum, sensible and latent heat, and enthalpy across the air-sea interface. These flux parameterizations will provide improved model coupling between the ocean and the atmosphere and, in essence, set the lower flux boundary conditions on atmospheric models and the upper flux boundary conditions on ocean models.

OBJECTIVES

1. Develop a physics-based framework for predicting air-sea fluxes from mean meteorological conditions and apply uniform analyses, based on this framework, to datasets that we will assemble.
2. Assemble a large collection of quality air-sea flux data that represents a wide variety of conditions.
3. Compute fluxes from these datasets using an improved analysis that better accommodates measurements made over heterogeneous surfaces, such as coastal zones. Focus the analyses on common problems where existing bulk formulations perform poorly—such as over surface heterogeneity, in weak winds, and in very strong winds.
4. Develop a unified algorithm for predicting the turbulent air-sea surface fluxes that spans the environmental range in our datasets and obeys theoretical principles.

APPROACH

This project—in its fourth year under ONR's Unified Parameterization Departmental Research Initiative—is a collaboration between Ed Andreas and Larry Mahrt. Dean Vickers of Oregon State University is a subcontractor on the project. Mahrt has focused on boundary-layer processes in weak winds, when stratification and surface heterogeneity are important issues, when turbulent fluxes are often hard to evaluate, and when models tend to perform poorly. Andreas, in contrast, has been concentrating on high winds, when sea spray is an important agent for heat and moisture transfer. Vickers brings expertise in processing large datasets—especially, aircraft data—and in parameterizing air-sea exchange. Together, we are developing flux parameterizations that span wind speeds from near zero to hurricane strength.

In outline, our flux algorithm is

$$\tau \equiv \rho u_*^2 = \rho\left[f\left(U_{N10}\right)\right]^2, \tag{1a}$$

$$H_{L,T} = H_{L,int} + H_{L,sp}, \tag{1b}$$

$$H_{s,T} = H_{s,int} + H_{s,sp}, \tag{1c}$$

$$Q_{en,T} = \left(H_{s,int} + H_{L,int}\right) + Q_{en,sp}. \tag{1d}$$

Here, τ is the surface stress or momentum flux; and $H_{L,T}$, $H_{s,T}$, and $Q_{en,T}$ are the *total* air-sea fluxes of latent heat, sensible heat, and enthalpy. These fluxes serve as the flux boundary conditions in atmospheric models and would be inserted at the lowest atmospheric modeling node.

In (1a), ρ is the air density, and u_* is the friction velocity. A key result of this project was our developing a new air-sea drag relation (Andreas et al. 2012). The $f(U_{N10})$ in (1a) represents this relation. Instead of obtaining the surface stress by parameterizing a drag coefficient or a roughness length (z_0), which is common practice in most air-sea flux algorithms (e.g., Smith 1988; Garratt 1992, p. 97–104; Fairall et al. 1996, 2003; Jones and Toba 2001), we estimate u_* directly from the neutral-stability, 10 m wind speed, U_{N10}.

In (1b)–(1d), the first term on the right side in each equation represents the *interfacial* flux (subscript int). Molecular processes right at the air-sea interface control these fluxes. Meanwhile, the second terms on the right in (1b)–(1d) represent the *spray-mediated* fluxes (subscript sp). Microphysics at the surface of the sub-millimeter spray droplets controls these fluxes. The left sides of (1) are total air-sea fluxes (subscript T)—presumably what is actually measured by eddy-covariance and the quantity that atmospheric models need at their lower boundary.

To develop this flux algorithm, we have assembled a large set of air-sea flux data and are still seeking other datasets. We currently have in hand 20 datasets comprising about 7000 air-sea flux measurements. In this set, surface-level wind speeds range from near zero to 72 m/s, and sea surface temperatures range from –1° to 32°C.

WORK COMPLETED

One of the main accomplishments of this last year was our writing and having accepted for publication a manuscript that describes our current version (Version 4.0) of a unified bulk air-sea flux algorithm (Andreas et al. 2014). We have also developed Fortran code for testing and implementing this algorithm. That code is freely available at www.nwra.com/resumes/andreas/software.php. Our previous annual reports and Andreas et al. (2012, 2014) describe details of both the interfacial and spray components of this algorithm. Here we show just Figures 1 and 2 to demonstrate the steps that we took in developing this algorithm.

Figure 1 presents scatter plots of the measured latent and sensible heat fluxes from our dataset and corresponding fluxes modeled with just the interfacial component of our flux algorithm. That is, the vertical axes in Figure 1 are $H_{L,int}$ and $H_{s,int}$. These figures test the null hypothesis: that an algorithm that recognizes only interfacial transfer can explain our data. In both panels in Figure 1, the measured fluxes, especially the larger fluxes, are larger than an algorithm that accounts for only interfacial transfer can explain. The null hypothesis fails.

Figure 2, in contrast, compares the same measurements in Figure 1 with modeled values that now include both interfacial and spray-mediated transfer, as parameterized in Andreas et al. (2014). Here, the fluxes collect much better about the 1:1 line. The bias values are evidence of the better results with the combined interfacial and spray model. In Figure 1, the measured-minus-modeled bias in the latent heat flux panel is 21.3 W/m^2 but is only 3.3 W/m^2 in Figure 2. Likewise, for the sensible heat flux panel in Figure 1, the bias is 8.6 W/m^2 but is only 1.0 W/m^2 in Figure 2. Clearly, modeled values that include individual parameterizations for both the interfacial and spray-mediated fluxes are necessary for representing the measurements.

As part of our work on weak wind regimes, we used the LongEZ aircraft data from the CBLAST Weak Wind Experiment to compute 100 m flight leg averages of turbulence quantities and the mean flow. We then related these turbulence fluxes and turbulent velocity scales to the wind speed and stratification through several stability parameters to look for relationships between wind speed and stratification in weak winds. We also extended this analysis to the three SHOWEX datasets (also collected by the LongEZ) and the RED data collected on FLIP that are in our data collection. We ultimately concluded that the approximately 30 m flight level used for the other aircraft data in our collection was too high for analyzing surface fluxes for weak wind and stable conditions. We are searching for additional datasets.

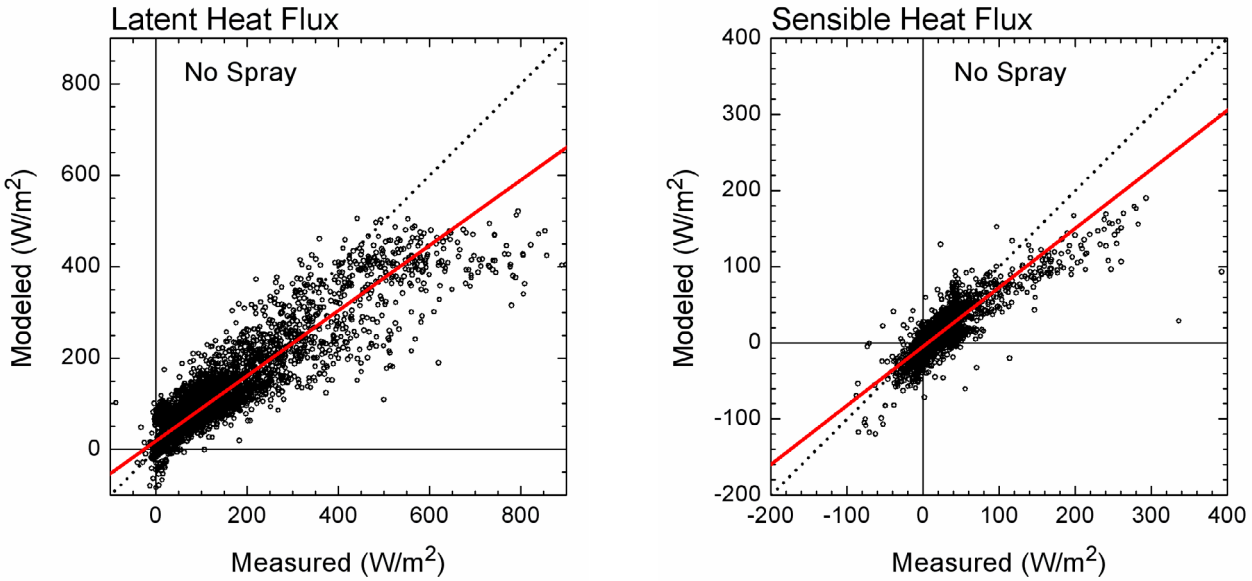

Figure 1. Tests of the null hypothesis. The two panels compare measurements of the latent and sensible heat fluxes against model values that come from just an interfacial flux algorithm. That is, the modeled values on the vertical axes include no spray-mediated flux contributions. In both panels, the dashed black line is 1:1, and the solid red line is the best fit through the data. In both panels, especially for large fluxes, the data points tend to fall under the 1:1 line; and the best-fit line, consequently, has a shallower slope. The results imply that measured fluxes, especially the large, positive heat fluxes, are larger than can be explained with an interfacial-only algorithm.

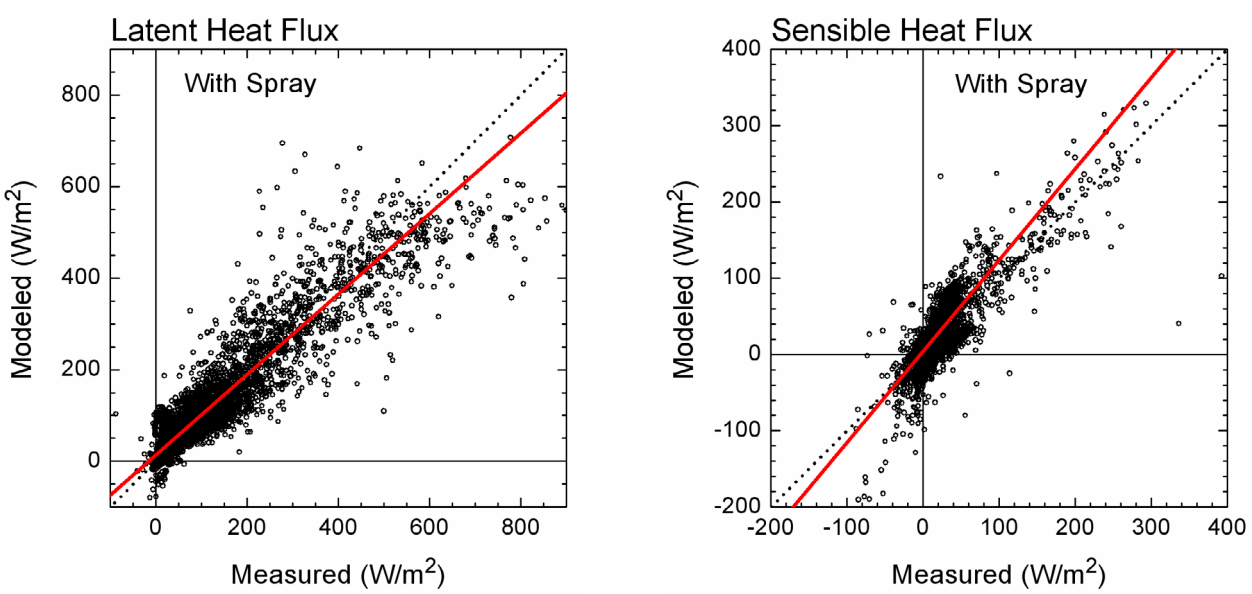

Figure 2. Scatter plots of latent and sensible heat fluxes as in Figure 1, but here the modeled fluxes include both interfacial and spray-mediated transfer as parameterized in Andreas et al. (2014). In both panels, the data cluster better about the 1:1 line than in Figure 1, and the red best-fit lines are closer to the 1:1 lines.

RESULTS

For the two flux routes represented in (1b)–(1d), we have physics-based parameterizations for each. In our view, this is the only way to represent fluxes measured in conditions when spray is plentiful. In other words, because the spray and interfacial fluxes scale so differently—e.g., the interfacial fluxes are approximately linear in wind speed while the spray fluxes are nearly cubic—their respective contributions to the measured fluxes cannot be separated with data analysis alone. But because we have theoretical predictions for both the spray and interfacial fluxes in (1b)–(1d), the analysis depicted in Figures 1 and 2 has essentially separated the spray and interfacial contributions in each measured flux.

The interfacial part of the algorithm is crucial in this analysis. Because we base our estimates of $H_{L,int}$ and $H_{s,int}$ on the COARE Version 2.6 algorithm (Fairall et al. 1996) that has been well verified in wind speeds up to 10 m/s (e.g., Grant and Hignett 1998; Chang and Grossman 1999), where spray contributes negligibly to the fluxes, we evaluate the spray fluxes for latent and sensible heat, for example, from (1) as

$$H_{L,sp} = H_{L,T} - H_{L,int}\,, \tag{2a}$$

$$H_{s,sp} = H_{s,T} - H_{s,int}\,. \tag{2b}$$

That is, we first estimate the spray contributions in the data by subtracting the estimated interfacial fluxes from the respective measured fluxes.
We do, nevertheless, also make physics-based estimates of $H_{L,sp}$ and $H_{s,sp}$ and compare these estimates with the data-based estimates. Andreas et al. (2014) report that the data-based estimate of $H_{L,sp}$ is, on average, only 2.5 times larger than the theoretical estimate. Considering the uncertainties and various approximations that are in the theoretical estimate of the spray flux, this is good agreement between data and theory.

For the spray sensible heat flux, on the other hand, Andreas et al. (2014) report that the data-based estimate of $H_{s,sp}$ is about 15 times larger than the corresponding theoretical estimate. Andreas et al. accounted for this discrepancy in their resulting bulk flux algorithm, but this mismatch is still disturbing.

As one explanation, Andreas et al. (2014) speculated that the larger sea spray droplets (spume droplets), which affect spray-mediated sensible heat transfer more than they do spray-mediated latent heat transfer, may not be accurately represented in the spray generation function that we used in making our theoretical estimates of $H_{L,sp}$ and $H_{s,sp}$. We will explore that possibility in the upcoming year.

In light of (2b), a second possible explanation for the discrepancy between the data-based and physics-based estimates of $H_{s,sp}$ is that the interfacial flux algorithm is not correct. To review, because of our new drag relation, (1a), our parameterizations for the interfacial fluxes are (Andreas et al. 2012, 2014)

$$H_{L,int} = \frac{\rho L_v k u_* \left(Q_s - Q_z\right)}{\ln\left(z/z_Q\right) - \psi_h\left(z/L\right)}\,, \tag{3a}$$

$$H_{s,int} = \frac{\rho c_p k u_* \left(\Theta_s - \Theta_z\right)}{\ln\left(z/z_T\right) - \psi_h\left(z/L\right)}\,. \tag{3b}$$

In these, L_v is the latent heat of vaporization; c_p, the specific heat of air at constant pressure; k (= 0.40), the von Kármán constant; Q_s and Θ_s, the specific humidity and potential temperature at the sea surface; and Q_z and Θ_z, the humidity and temperature at height z. In addition, ψ_h is a stratification correction that is a known function of z/L, where L is the Obukhov length.

The most crucial variables in (3) are the roughness lengths for humidity (z_Q) and temperature (z_T). For these, we have been using the parameterization that Liu et al. (1979) derived from surface-renewal theory. This is the same parameterization used in the COARE Version 2.6 algorithm (Fairall et al. 1996). But with the concerns we have over estimating the spray sensible heat flux, we have recently been reevaluating this choice.

By replacing the interfacial latent and sensible heat fluxes in (3) with the corresponding total measured fluxes ($H_{L,T}$ and $H_{s,T}$), we can invert (3a) and (3b) and thereby evaluate z_Q and z_T from data under the assumption that all air-sea transfer obeys interfacial scaling. Figure 3 shows our calculations.

Both panels in Figure 3 suggest two alternative interpretations. The z_Q values tend to follow the COARE 2.6 curve up to about 11 m/s but then drift higher—evidence of spray-mediated transfer that does not obey interfacial scaling. In the z_T panel, the data tend to follow the COARE 2.6 curve up to about 14 m/s but then also drift higher when spray-mediated sensible heat transfer becomes significant. Alternatively, if either the Garratt (1992) or Andreas (1987) model is the proper parameterization for z_Q and z_T, the data in Figure 3 follow interfacial scaling up to about 17 m/s before drifting higher because of spray-mediated transfer.

Clearly, these are very different interpretations. But knowing which parameterization for z_Q and z_T is correct is crucial to our spray analysis because of our approach, (2), where the magnitude of the spray flux is intimately tied to the estimated magnitude of the interfacial flux. In the next year, we will investigate further which theoretical model for z_Q and z_T is most consistent with our data.

As an instructive investigation of Monin Obukhov similarity theory, we constructed a simple model based on a third-order polynomial that predicts the friction velocity from the wind speed in near-neutral conditions. An additional function based on the bulk Richardson number applies a correction for stability. The model coefficients are tuned using data from four different aircraft in nine different experiments comprising 5000 observations that are in our combined dataset.

We did not correct the independent variable, wind speed, for height or stability but instead used the measured value of the mean wind speed in the third-order polynomial. We also did not standardize the wind speed to a constant height, say 10 m, as is typically done in observational studies because doing so would require introducing the quantity that we are estimating, friction velocity, into the independent variable, wind speed. The simple model does not require an estimate of the Obukhov length or the aerodynamic roughness length, both of which are subject to large uncertainty; and it does not require iteration.

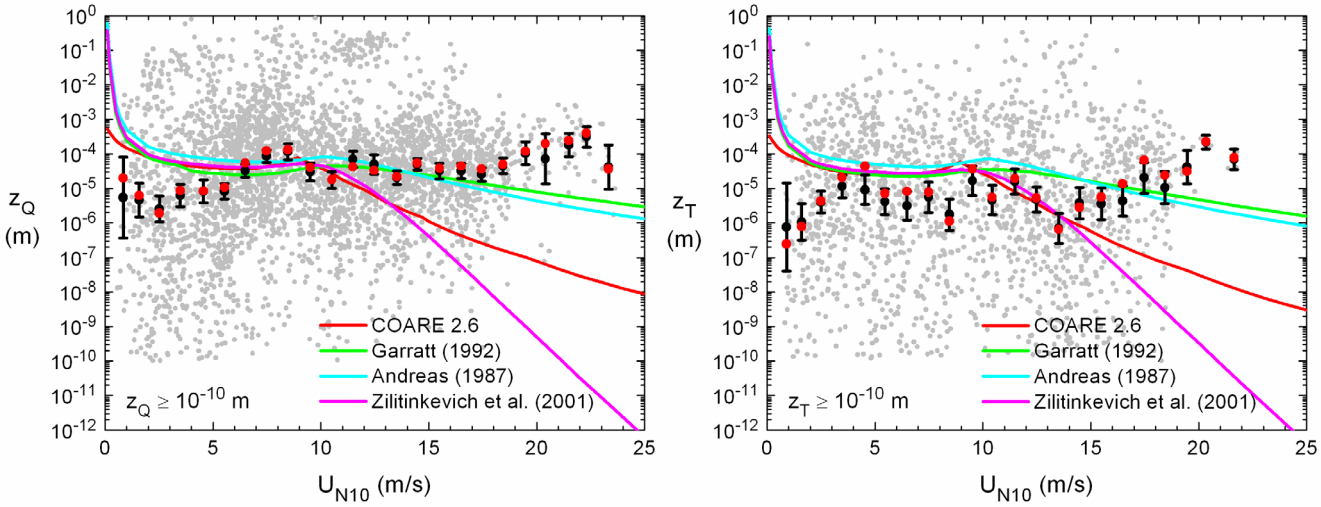

Figure 3. Estimates of the roughness lengths for humidity and temperature, z_Q and z_T, from our datasets are plotted versus the neutral-stability wind speed at 10 m, U_{N10}. The black circles are bin averages in bins that are 1 m/s wide in U_{N10}; the error bars are ±2 standard deviations in these bin averages. The red circles, which generally agree with the averages, are medians in these same bins. Each panel also shows four curves that are theoretical predictions for these roughness lengths. The COARE 2.6 curves are from Version 2.6 of the COARE algorithm (Fairall et al. 1996; Liu et al. 1979) and parameterize the interfacial fluxes in our current algorithm (Andreas et al. 2014). The Garratt (1992, p. 90–93), Andreas (1987), and Zilitinkevich et al. (2001) curves, like Liu et al. (1979), are based on surface-renewal theory or scaling arguments. At wind speeds up to 10 m/s, all four theoretical estimates predict similar roughness lengths. At higher wind speeds, the Zilitinkevich et al. model predicts values that are unrealistically small. The Garratt and Andreas models predict the largest values at high winds; the COARE 2.6 curves are midway between these two extremes.

The friction velocities from this simple model and those from the COARE scheme (Fairall et al. 1996), based on a full implementation of Monin-Obukhov similarity theory and the Charnock relation, compare well to the observations. Similar close agreement was found between the simple model and a recently published formulation of the friction velocity based on a linear dependence on U_{N10} (i.e., Andreas et al. 2012). In addition, the simple model was effective in predicting the friction velocity for three independent datasets. This work shows that discarding the complexity of Monin-Obukhov similarity theory and avoiding the large uncertainty in estimating the Obukhov length and the roughness length can lead to a credible model for the friction velocity for most situations. A manuscript describing this work is in review (Vickers et al. 2014).

After realizing the potential of the simple approach in Andreas et al. (2012), where the surface friction velocity was related directly to the wind speed alone, we launched a more extensive analysis of this approach. We first recognized that stable boundary layers over the sea can be particularly thin, sometimes less than 20 m deep. The surface layer, nominally the lowest 10% of the boundary layer, is then too thin to be observed with aircraft. Even weakly stable boundary layers may be less than 100 m deep—in which case, using fluxes at the standard 30 m flight level is not formally justified.

Consequently, the following analysis, which continues our work on weak winds, emphasizes the LongEZ aircraft data taken in the CBLAST Weak Wind Pilot Experiment and in three SHOWEX field programs. Although the LongEZ flew at a variety of levels, we used just legs that were at 13 m and lower.

Several turbulent velocities scales, denoted u_t, were related to the mean wind speed (Figure 4). The goal here is to assess whether various measures of the turbulence have the same dependence on wind speed or whether that dependence reflects how the turbulence is represented. The 100 m flight leg values of the turbulent velocities for flight legs lower than 13 m above the sea were averaged for different intervals of the wind speed for all of the cases with stable conditions where the heat flux is downward and $\delta\theta > 0.1$ K. Here, $\delta\theta$ is the air-minus-sea temperature difference. As velocity scales u_t, the figure shows standard deviations in horizontal (σ_v) and vertical (σ_w) velocities, u_* computed two ways, and

$$V_{w\theta} = -\frac{H_{s,T}}{\rho c_p \sigma_\theta}, \tag{4}$$

where σ_θ is the standard deviation in air temperature.

The different turbulent velocity scales differ substantially in overall magnitude. For easier comparison of the dependencies on wind speed, we normalized the turbulent velocity scales in Figure 4 by the value in the interval of highest wind speed. The shapes with respect to wind speed of the resulting nondimensional functions do not depend significantly on this choice.

Figure 4 indicates that the dependence of the scaled turbulent velocities on the wind speed exhibits a stronger slope for winds greater than about 6 m/s. The change of slope is well defined considering that the 100 m averages represent different values of stability, wave states, and measurement height. All five turbulent velocity scales are characterized by this slope transition. The within-interval standard deviation is largest at the weakest wind speeds, where it reaches about 10% of the interval averages.

For weaker winds, the turbulence is thought to be fine scale and possibly related to aerodynamically smooth flow conditions. For winds higher than the transition at about 6 m/s, the turbulence is like fully rough flow and is dominated by bulk shear instability and coherent structures such as roll vortices. Existing similarity theory and the usual bulk formula do not include this transition, but our new drag relation (Andreas et al. 2012) recognizes aerodynamically smooth and rough flow and the transition between the two regimes.

The turbulence decreases with increasing stratification but substantially more slowly than predicted by similarity theory. The dependence of the turbulent velocities on wind speed for two classes of stratification shows only small differences (Figure 5) despite the fact that the stratification for the solid lines is double that for the dashed lines. The role of stratification is, therefore, secondary in setting turbulence levels and may be masked by other influences, such as wave state, fetch dependence, and a near-surface wind maximum. We are still investigating the reasons for the weak dependence of the turbulence on stratification.

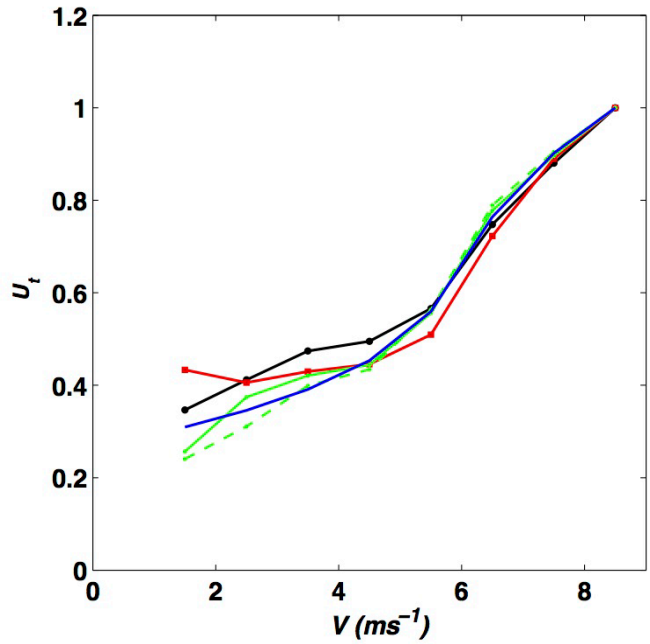

Figure 4. Bin-averaged turbulent velocities scaled by the respective velocities in the interval of highest wind speed; the vertical axis is therefore nondimensional. The velocity scales shown, all denoted u_t, are standard deviation in horizontal velocity (σ_v, blue), standard deviation in vertical velocity (σ_w, black), interval averages of the magnitudes of the friction velocity (u_*, solid green), and $V_{w\theta}$ (red, see definition in (4)) as functions of bin-averaged wind speed, V. The green dashed line is the friction velocity derived from interval-averaged flux components in an along-wind coordinate system. All five scales show shallow slopes that increase with wind speed for wind speeds below about 6 m/s. This region is probably indicative of aerodynamically smooth flow. Above 6 m/s, as the flow transitions to aerodynamically rough flow, all five velocity scales increase more rapidly with wind speed.

Stable boundary layers over the sea are generally related to advection of warm air (often from land) over cooler water. This advection leads to a much weaker relationship between the wind speed and stratification than we see in stable boundary layers over land. Over the sea, the wind attempts to decrease the stratification through shear-induced mixing but also acts to increase startification through warm-air advection. The turbulence is found to increase systematically with the product of the wind speed and the stratification in contrast to stable boundary layers over land.

IMPACT/APPLICATIONS

One of our goals is to develop Fortran code for a bulk air-sea flux algorithm that provides a unified treatment of fluxes for winds from near zero to hurricane strength. Of necessity, for treating high winds, this code must account for spray-mediated transfer. In the last year, we finalized that code, Version 4.0 of our flux algorithm, and have a paper in press that describes it (Andreas et al. 2014).

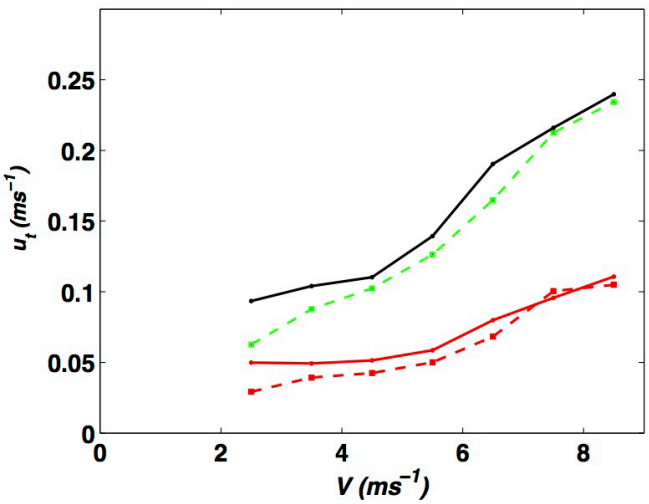

Figure 5. The dependence of u_* (black, green) and $V_{w\theta}$ (red) (both denoted as u_t) on bin-averaged wind speed for $\delta\theta > 1.8$ K (dashed) and $\delta\theta < 1.5$ K (solid). Although the levels of the two velocity scales are different, both behave as in Figure 4; they have shallower slopes for wind speeds below 6 m/s and steeper slopes above this transition velocity. Moreover, the levels and slopes depend only weakly on the temperature difference—the stratification.

An application for this work is for coupling atmosphere and ocean in regional and global models. As such, we have provided our new code to interested parties in the U.S. and Europe. In particular, we provided the code to modelers at NRL-Monterey, and Jim Ridout at NRL has been testing it in the Navy's global model, NAVGEM.

TRANSITIONS

Journal articles and conference presentations document our work on air-sea exchange. Andreas has also developed a software "kit" that contains instructions, supporting documents, and the Fortran programs necessary to implement the bulk air-sea flux algorithm described by Andreas et al. (2012, 2014). The current version of that code is 4.0, and the kit is posted at http://www.nwra.com/resumes/andreas/software.php, where it can be freely downloaded.

As mentioned above, we have also sent this code directly to modelers at NRL-Monterey for their testing and evaluation.

RELATED PROJECTS

Andreas and Kathy Jones of the Army's Cold Regions Research and Engineering Laboratory started in FY12 a project to study spray icing of offshore structures that is funded under ONR's Arctic program. In January 2013, we carried out a month-long field program on Mt. Desert Rock, a small, well-exposed island 24 miles out into the Atlantic from Bar Harbor, Maine (Jones and Andreas 2013).

During that experiment, we made continuous measurements of spray droplet concentrations with a cloud imaging probe that could count and size droplets in 12.5 μm radius bins from near 0 μm to

755 µm. Figure 6 shows quality-controlled spectra that we measured when the wind speed was 13–14 m/s. From these and many similar spectra at other wind speeds, we expect to test and revise our formulation for the spray generation function. Because the spray generation function is also crucial in our current project, this related project that ONR's Arctic program supports nicely complements it.

In June 2014, Andreas began a collaborative project with Penny Vlahos and Ed Monahan at the University of Connecticut to study spray-mediated air-sea gas transfer. The National Science Foundation is funding this work. Briefly, ocean scientists have been investigating bubble-mediated air-sea gas transfer for over 30 years, but no one has yet looked at the mirror-image process of spray-mediated air-sea gas transfer. This NSF project will complement and build on Andreas's current work for ONR because, to estimate the rate of spray-mediated gas transfer, we will also need to know the spray generation function. And, as with spray-mediated heat transfer, microphysics in and around spray droplets controls how efficient the droplets are in transferring gases between the ocean and the atmosphere.

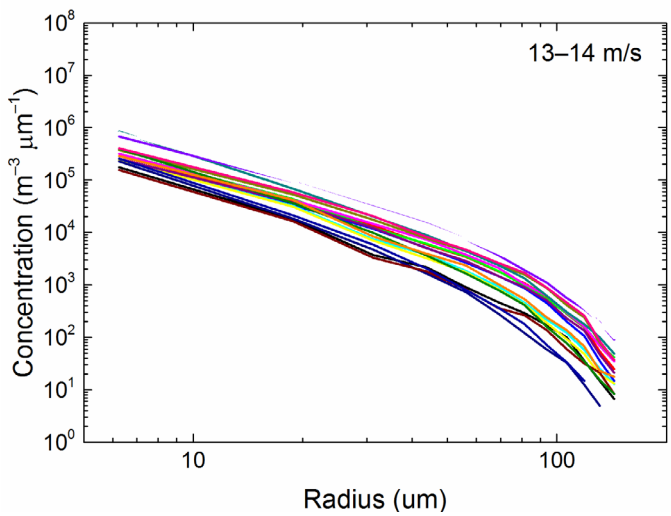

Figure 6. Eighteen spray droplet concentration spectra measured with a cloud imaging probe on Mt. Desert Rock, a small island 24 miles out into the Atlantic from Bar Harbor, Maine. The units of concentration are number of droplets per cubic meter of air per micrometer increment in droplet radius. The wind speeds during these measurements were 13–14 m/s, and the radii plotted range from bins centered at 6.75 µm to 143.75 µm. All 18 curves have essentially the same shape and agree in the concentration at a given radius to within an order of magnitude. In the nearly linear region of this log-log plot, concentration decreases approximately as the inverse radius cubed (i.e., as r^{-3}).

REFERENCES

Andreas, E. L, 1987: A theory for the scalar roughness and the scalar transfer coefficients over snow and sea ice. *Bound.-Layer Meteor.*, **38**, 159–184.

Andreas, E. L, L. Mahrt, and D. Vickers, 2012: A new drag relation for aerodynamically rough flow over the ocean. *J. Atmos. Sci.*, **69**, 2520–2537.

Andreas, E. L, L. Mahrt, and D. Vickers, 2014: An improved bulk air-sea surface flux algorithm, including spray-mediated transfer. *Quart. J. Roy. Meteor. Soc.*, **140**, in press.

Chang, H.-R., and R. L. Grossman, 1999: Evaluation of bulk surface flux algorithms for light wind conditions using data from the Coupled Ocean-Atmosphere Response Experiment (COARE). *Quart. J. Roy. Meteor. Soc.*, **125**, 1551–1588.

Fairall, C. W., E. F. Bradley, D. P. Rogers, J. B. Edson, and G. S. Young, 1996: Bulk parameterization of air-sea fluxes for Tropical Ocean-Global Atmosphere Coupled-Ocean Atmosphere Response Experiment. *J. Geophys. Res.*, **101**, 3747–3764.

Fairall, C. W., E. F. Bradley, J. E. Hare, A. A. Grachev, and J. B. Edson, 2003: Bulk parameterization of air-sea fluxes: Updates and verification for the COARE algorithm. *J. Climate*, **16**, 571–591.

Garratt, J. R., 1992: *The Atmospheric Boundary Layer.* Cambridge University Press, 316 pp.

Grant, A. L. M., and P. Hignett, 1998: Aircraft observations of the surface energy balance in TOGA-COARE. *Quart. J. Roy. Meteor. Soc.*, **124**, 101–122.

Jones, I. S. F., and Y. Toba, Eds., 2001: *Wind Stress over the Ocean.* Cambridge University Press, 307 pp.

Jones, K. F., and E. L Andreas 2013: Winter measurements of sea spray at Mt. Desert Rock. *Proc. 15th International Workshop on Atmospheric Icing of Structures (IWAIS XV)*, St. John's, Newfoundland, 8–11 September 2013, 3-48–3-53.

Liu, W. T., K. B. Katsaros, and J. A. Businger, 1979: Bulk parameterization of air-sea exchanges of heat and water vapor including the molecular constraints at the interface. *J. Atmos. Sci.*, **36**, 1722–1735.

Smith, S. D., 1988: Coefficients for sea surface wind stress, heat flux, and wind profiles as a function of wind speed and temperature. *J. Geophys. Res.*, **93**, 15,467–15,472.

Vickers, D., L. Mahrt, and E. L Andreas, 2014: Formulations of the sea-surface friction velocity in terms of the mean wind and bulk stability. *J. Appl. Meteor. Climatol.*, submitted.

Zilitinkevich, S. S., A. A. Grachev, and C. W. Fairall, 2001: Scaling reasoning and field data on the sea surface roughness lengths for scalars. *J. Atmos. Sci.*, **58**, 320–325.

PUBLICATIONS

Andreas, E. L, 2012: Book review: *Time Series Analysis in Meteorology and Climatology: An Introduction*. *Bulletin of the American Meteorological Society*, **93**, 1417–1419. [published]

Andreas, E. L, 2014: Perspectives on estimating the spray-mediated flux of gases across the air-sea interface. Extended abstract, *16th Conference on Atmospheric Chemistry*, Atlanta, GA, 3–6 February 2014, American Meteorological Society, paper 7.1, 11 pp. [published]

Andreas, E. L, R. E. Jordan, L. Mahrt, and D. Vickers, 2012: More on the Bowen ratio over saturated surfaces. Extended abstract, *20th Symposium on Boundary Layers and Turbulence*, Boston, MA, 9–13 July 2012, American Meteorological Society, paper 14A.3, 10 pp. [published]

Andreas, E. L, L. Mahrt, and D. Vickers, 2012: A new drag relation for aerodynamically rough flow over the ocean. *Journal of the Atmospheric Sciences*, **69**, 2520–2537. [published, refereed]

Andreas, E. L, L. Mahrt, and D. Vickers, 2012: A new drag relation for aerodynamically rough flow over the ocean. Extended abstract, *18th Conference on Air-Sea Interaction*, Boston, MA, 9–12 July 2012, American Meteorological Society, paper 3.2, 19 pp. [published]

Andreas, E. L, R. E. Jordan, L. Mahrt, and D. Vickers, 2013: Estimating the Bowen ratio over the open and ice-covered ocean. *Journal of Geophysical Research Oceans*, **118** (9), 4334–4345. doi:10.1002/jgrc.20295. [published, refereed]

Andreas, E. L, L. Mahrt, and D. Vickers, 2014: An improved bulk air-sea surface flux algorithm, including spray-mediated transfer. Extended abstract, *21st Symposium on Boundary Layers and Turbulence*, Leeds, U.K., 9–13 June 2014, American Meteorological Society, paper 2B.3, 19 pp. [published]

Andreas, E. L, L. Mahrt, and D. Vickers, 2014: An improved bulk air-sea surface flux algorithm, including spray-mediated transfer. *Quarterly Journal of the Royal Meteorological Society*, **140**. [in press, refereed]

Jones, K. F., and E. L Andreas, 2012: Sea spray concentrations and the icing of fixed offshore structures. *Quarterly Journal of the Royal Meteorological Society*, **138**, 131–144. [published, refereed]

Mahrt, L., D. Vickers, E. L Andreas, and D. Khelif, 2012: Sensible heat flux in near-neutral conditions over the sea. *Journal of Physical Oceanography*, **42**, 1134–1142. [published, refereed]

Mahrt, L., D. Vickers, and E. L Andreas, 2014: Low-level wind maxima and structure of the stably stratified boundary layer in the coastal zone. *Journal of Applied Meteorology and Climatology*, **53**, 363–376. [published, refereed]

Vickers, D., L. Mahrt, and E. L Andreas, 2013: Estimates of the 10-m neutral sea surface drag coefficient from aircraft eddy-covariance measurements. *Journal of Physical Oceanography*, **43**, 301–310. [published, refereed]

Vickers, D., L. Mahrt, and E. L Andreas, 2014: Formulations of the sea-surface friction velocity in terms of the mean wind and bulk stability. *Journal of Applied Meteorology and Climatology*. [refereed]

HONORS/AWARDS/PRIZES

Ed Andreas was introduced as a new Fellow of the American Meteorological Society at the AMS Annual Meeting in Atlanta in February 2014.